Original Article

BIOENGINEERED GREEN-SYNTHESIZED TITANIUM DIOXIDE AND CHITOSAN NANOPARTICLE-MODIFIED GLASS IONOMER CEMENT: ANTIMICROBIAL, MECHANICAL, AND SURFACE PROPERTIES EVALUATION

Soorya Ganesh[1], Jessy Paulraj[1], Subhabrata Maiti[2]*

[1]*Department of Pediatric and Preventive Dentistry, Saveetha Dental College and Hospitals, Saveetha Institute of Medical and Technical Sciences (SIMATS), Saveetha University, Chennai-77, India. drjessy2019@gmail.com*
[2]*Department of Prosthodontics, Saveetha Dental College and Hospitals, Saveetha Institute of Medical and Technical Sciences (SIMATS), Saveetha University, Chennai-77, India.*

Received: 23 January 2026; **Revised:** 01 April 2026; **Accepted:** 04 April 2026 https://doi.org/10.51847/MRLJvvlef7

ABSTRACT

To synthesize and characterize green-mediated titanium dioxide– and chitosan-modified glass ionomer cement and compare their antimicrobial, mechanical, and surface properties with conventional GIC. Titanium dioxide nanoparticles were synthesized using Azadirachta indica extract and incorporated into GIC to produce TiO_2-GIC. Chitosan-modified GIC (Chi-GIC) was prepared using chitosan synthesized with Eucalyptus globulus extract. Three groups were evaluated: TiO_2-GIC, Chi-GIC, and conventional GIC (control). Characterization was performed using Fourier transform infrared spectroscopy, scanning electron microscopy, and energy-dispersive X-ray spectroscopy. Specimens were tested for antimicrobial activity, surface roughness, microhardness, and compressive strength. Data were analyzed using one-way ANOVA and Tukey post-hoc tests ($p < 0.05$). Chi-GIC showed the highest antibacterial activity against *Streptococcus mutans* (19.37 ± 1.24 mm) and *Lactobacillus acidophilus* (18.41 ± 1.19 mm), followed by TiO_2-GIC and conventional GIC. TiO_2-GIC exhibited the highest microhardness (78.42 ± 3.15 VHN) and compressive strength (165.42 ± 8.36 MPa) with the lowest surface roughness (0.82 ± 0.07 µm). Nanoparticle incorporation significantly improved properties ($p < 0.05$). Green-mediated incorporation of titanium dioxide nanoparticles and chitosan significantly enhanced GIC performance. TiO_2-GIC improved mechanical properties, whereas Chi-GIC demonstrated superior antibacterial activity.

Key words: Glass ionomer cement, Greenhouse, Titanium dioxide nanoparticles, Chitosan, Antimicrobial activity, Mechanical properties.

Introduction

Glass ionomer cement (GIC) is widely utilized in restorative dentistry because of its ability to chemically adhere to enamel and dentin, release fluoride over time, exhibit good biocompatibility, and allow easy clinical manipulation [1]. Owing to these favorable characteristics, GIC is frequently employed in atraumatic restorative treatment (ART), pediatric and geriatric dentistry, and in the management of patients with high caries risk [2, 3]. However, despite these advantages, the clinical performance of conventional GIC is restricted by its relatively poor mechanical properties, such as low compressive strength, limited fracture toughness, reduced surface hardness, and a high susceptibility to wear and moisture contamination during the early stages of setting [4].

To address the inherent limitations of conventional GIC, several modification strategies have been investigated, including the incorporation of metal powders, fibers, bioactive glasses, and nanoparticles. Among these approaches, nanoparticle reinforcement has attracted considerable attention due to its potential to improve mechanical performance while maintaining the intrinsic benefits of GIC. Titanium-based nanoparticles, in particular, are recognized for their superior mechanical strength, corrosion resistance, biocompatibility, and notable antimicrobial activity [5]. The incorporation of titanium nanoparticles into the GIC matrix enhances stress distribution within the material and contributes to improved resistance to crack initiation and propagation [5].

In recent years, the green synthesis of nanoparticles using plant extracts has gained attention as an environmentally friendly and biologically safe alternative to conventional chemical synthesis methods [6-13]. Neem (*Azadirachta indica*), a member of the Meliaceae family, is widely recognized for its numerous therapeutic properties [14]. Plant-derived products are increasingly favored due to their biodegradability, low toxicity to non-target organisms, cost-effectiveness, and wide availability. In traditional Indian medicine, neem has long been valued as a rich source of medicinal compounds [15]. Extracts obtained from *Azadirachta indica* possess notable antibacterial activity, and dried neem chewing sticks have demonstrated strong inhibitory effects against *Streptococcus mutans* compared with other cariogenic microorganisms [15]. These properties make neem a promising candidate for the green synthesis of titanium nanoparticles. Neem-mediated titanium nanoparticles have been reported to exhibit

enhanced bioactivity and improved interaction with dental restorative materials.

Chitosan is a naturally derived polymer produced through the alkaline N-deacetylation of chitin, which is obtained from crustacean shells such as those of crabs, shrimps, and lobsters. It is widely recognized for its non-toxic, biocompatible, and biodegradable nature. Chitosan exhibits a wide range of biological properties, including antifungal, antibacterial, antiprotozoal, anticancer, antiplaque, antitartar, and hemostatic activities [16]. Due to these favorable characteristics, nanoscale chitosan formulations have been extensively explored in pharmacology, particularly as drug delivery systems [16]. Petri *et al*. investigated chitosan-modified glass ionomer cement by incorporating chitosan at different concentrations (10, 20, and 30 wt.%) into the GIC matrix [17].

The incorporation of plant extracts such as *Eucalyptus globulus* during the preparation of chitosan can further enhance its antimicrobial efficacy owing to the presence of various bioactive phytochemicals [18-27]. Eucalyptus leaf extract has been considered a promising alternative due to its broad-spectrum antimicrobial activity against several oral pathogens [28]. Eucalyptus oil has also been reported to serve as an adjunctive agent in reducing bacteria associated with dental caries and endodontic infections [29]. Mohammed demonstrated that the methanolic extract of eucalyptus leaves exhibited stronger inhibitory effects against *Streptococcus mutans*, a primary causative microorganism in dental caries, compared with conventional antimicrobial agents such as gentamicin and nystatin [30]. Similarly, another study reported that extracts obtained from eucalyptus twigs showed significant antimicrobial activity against *S. mutans* [31]. Despite these promising findings, the incorporation of eucalyptus leaf extract into dental restorative materials has not been extensively investigated.

Although numerous studies have investigated individual modifications of glass ionomer cement, limited literature is available that directly compares green-synthesized titanium-modified GIC with plant extract–enhanced chitosan-modified GIC within a single experimental framework. Therefore, the present in vitro study was conducted to comparatively assess the antimicrobial efficacy, mechanical properties, and surface characteristics of green-mediated titanium-modified GIC and green-mediated chitosan-modified GIC in comparison with conventional GIC. It was hypothesized that Neem-mediated titanium-modified GIC would exhibit superior performance, followed by chitosan-modified GIC, while conventional GIC would demonstrate comparatively lower properties.

Materials and Methods

Estimation of sample size, study design, and materials

Sample size estimation was performed using the G*Power statistical software, considering a statistical power of 0.95 (95% confidence level) and an effect size of 0.6, which indicated that a total of 48 samples were required for each parameter. The glass ionomer cement used in this study consisted of aluminosilicate glass powder and polyacrylic acid (GC Corporation, Tokyo, Japan). Dried neem and eucalyptus leaves were procured from Annai Aravindh Herbals Pvt. Ltd., Chennai, India. Zirconium oxide was obtained from Sigma-Aldrich Chemicals Private Limited, Bengaluru, India. The present in vitro experimental study was carried out at the research center of the university hospital.

Preparation of green-mediated titanium dioxide nanoparticles and incorporation into the GIC

Green-mediated titanium oxide nanoparticles were synthesized using *Azadirachta indica* (neem) leaf extract. All glassware was cleaned, sterilized, and dried. Fresh leaves were washed, shade-dried, and 1 g was boiled in 100 mL distilled water for 5–10 minutes. The extract was cooled and filtered (Whatman No.1). Separately, 0.365 g TiO_2 was dissolved in 50 mL distilled water to prepare the precursor **(Figure 1a)**. Neem extract was added gradually under magnetic stirring, then incubated at 37 °C to facilitate nanoparticle formation **(Figure 1b)**. The synthesized nanoparticles were incorporated into GIC at 5% (Group I). The GIC powder and nanoparticles were weighed, vortex-mixed for uniformity, and combined with the liquid component following the manufacturer's powder–liquid ratio.

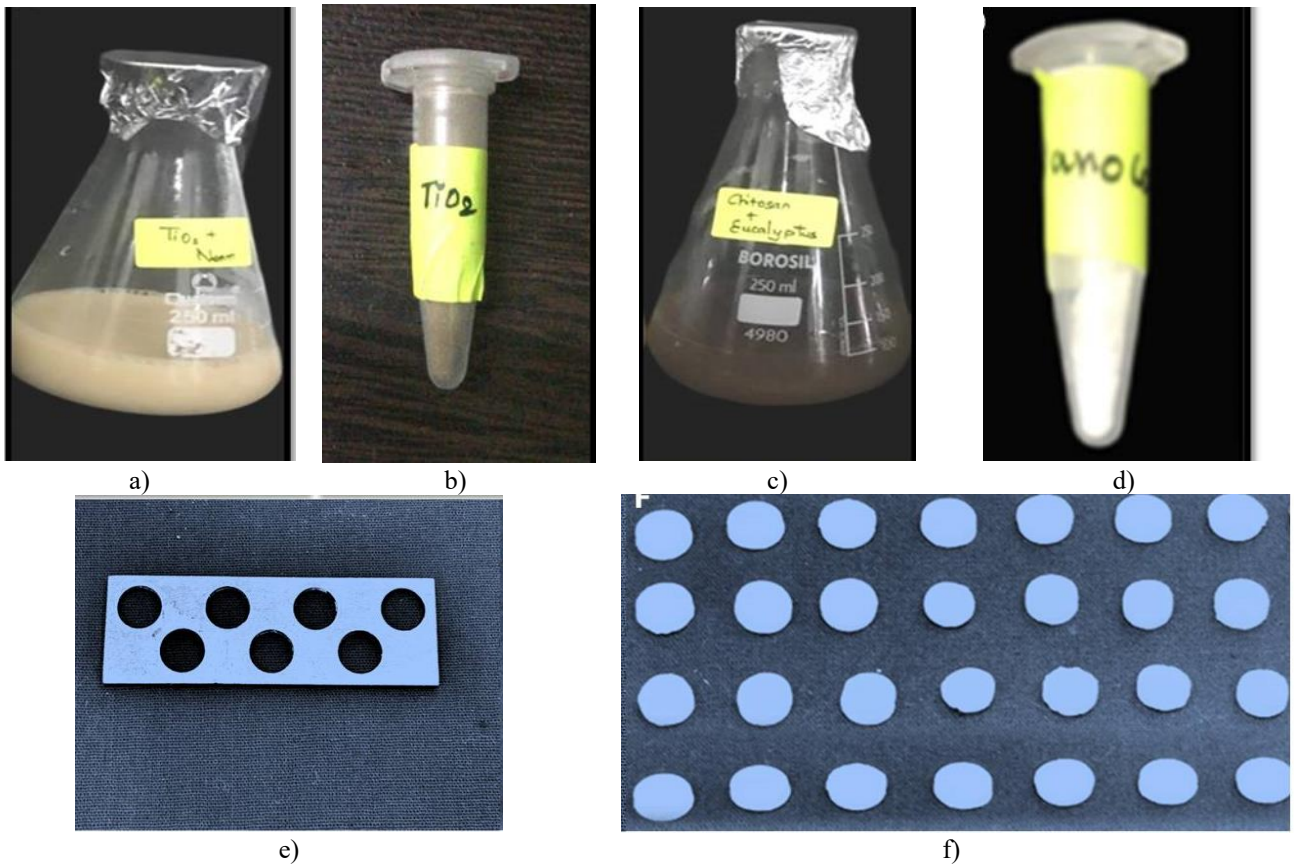

Figure 1. Preparation of nanoparticles and specimen fabrication. a) Preparation of titanium dioxide (TiO_2) nanoparticles using the green synthesis method. b) Final TiO_2 nanoparticle precipitate obtained after synthesis and processing. c) Preparation of chitosan nanoparticles using the green synthesis d) Final form of chitosan nanoparticles obtained after processing. e) Stainless steel mold used for specimen fabrication. f) Prepared specimens used for experimental testing.

Preparation of green -mediated chitosan nanoparticles and incorporation into the GIC

Green-mediated chitosan nanoparticles were synthesized using *Eucalyptus globulus* leaf extract. Leaves were washed, shade-dried, and 1 g was heated in 100 mL distilled water at 60–80 °C for 5–10 minutes. The extract was cooled and filtered (Whatman No.1). Chitosan solution was prepared by dissolving 0.5 g chitosan in 0.5 g glacial acetic acid and 49 mL distilled water under stirring. Then, 4–5 drops of sodium tripolyphosphate (TPP) were added for ionic gelation. The eucalyptus extract was gradually added with constant stirring **(Figure 1c)**, followed by incubation at 37 °C to form nanoparticles **(Figure 1 parts d,e,f)**. The synthesized nanoparticles were incorporated into GIC at 5% (Group II). Chitosan was added to the liquid component to prepare a 5% modified liquid, and then mixed with GIC powder as per the manufacturer's ratio to obtain homogeneous cement.

Fourier Transform Infrared (FTIR) analysis

Fourier Transform Infrared Spectroscopy (FTIR) was used to evaluate the chemical changes following the incorporation of titanium nanoparticles and chitosan into glass ionomer cement. The spectra were recorded using an FTIR spectrometer (Nicolet iS10; Thermo Fisher Scientific, Waltham, Massachusetts, USA) over a wavelength range of 500–4000 cm^{-1} with a resolution of 4 cm^{-1}. This analysis was performed to identify the characteristic functional groups present in the modified GIC powders and to assess potential chemical interactions between the nanoparticles and the conventional GIC matrix.

Scanning Electron Microscopy (SEM) analysis

The microstructure of titanium nanoparticle–modified and chitosan-modified glass ionomer cement (GIC) powders was analyzed using scanning electron microscopy (SEM) (JEOL JSM IT-800, Germany). Prior to analysis, the powder samples were mounted on aluminum stubs and sputter-coated with a thin layer of gold to improve electrical conductivity. The coating was performed at a gas pressure of approximately 50 mTorr and a current of about 40 mA for 180 seconds. The coated specimens were then examined under SEM to evaluate the surface morphology and particle distribution of the modified GIC powders.

Energy Dispersive X-ray (EDX) analysis

Energy Dispersive X-ray Spectroscopy (EDX) was employed to analyze the elemental composition of the

cement samples. The specimens were prepared in powder form and examined using an EDX system manufactured by FEA Company of USA (S.E.A) PTE LTD. The detected elements were quantified and expressed as weight percentages (wt%), with values reported up to two decimal places for accuracy.

Grouping of samples

The samples were categorized into three experimental groups according to the type of modification incorporated into the glass ionomer cement. Group I included titanium-modified GIC, prepared by adding 5% (w/w) titanium nanoparticles to the conventional GIC powder. Group II consisted of chitosan-modified GIC, in which 5% (w/w) chitosan was incorporated into the cement. Group III served as the control group and comprised conventional glass ionomer cement without any modification.

Specimen preparation

Type IX glass ionomer cement (GIC) (GC Corporation, Tokyo, Japan) was used for specimen preparation. For the experimental groups, green-mediated titanium nanoparticles were incorporated into the conventional GIC powder at a concentration of 5% (w/w). The modified powder was mixed with the polyacrylic acid–based liquid component (GC Corporation) according to the manufacturer's recommended powder-to-liquid ratio to obtain a homogeneous paste. The mixture was then transferred into cylindrical molds measuring 5 mm in diameter and 2 mm in thickness using a sterile cement carrier and gently leveled with a sterile glass slide to produce a uniform surface. Similarly, green-mediated chitosan-modified GIC specimens were prepared by incorporating 5% (w/w) chitosan into the cement following the same procedure. After the setting reaction was complete, all specimens were inspected under bright illumination for defects such as porosities, voids, or cracks, and any defective samples were discarded. The accepted specimens were subsequently finished, polished, and stored at room temperature until further evaluation.

Evaluation of antibacterial activity

The antibacterial activity of the experimental materials was assessed against *Streptococcus mutans* and *Lactobacillus acidophilus* using the agar well diffusion method. Bacterial suspensions were uniformly spread onto Mueller–Hinton agar plates, and wells of approximately 6 mm in diameter were created using a sterile cork borer. Specimens from Group I (5% green-mediated titanium nanoparticle–modified GIC), Group II (5% green-mediated chitosan nanoparticle–modified GIC), and Group III (conventional GIC) were placed into the prepared wells and incubated at 37 °C for 24 hours. Following incubation, the zones of inhibition formed around the specimens were measured in millimeters using a digital vernier caliper, and the mean values were recorded for subsequent statistical analysis.

Evaluation of surface roughness

The surface roughness of the prepared specimens was assessed using a surface profilometer. Prior to analysis, all specimens were finished and polished to ensure a standardized and smooth surface. Each sample was positioned on the profilometer stage, and a stylus was traversed across the specimen surface under controlled conditions to record surface irregularities. The instrument measured the average surface roughness (Ra) values in micrometers (μm). For each specimen, three measurements were obtained at different locations, and the mean value was calculated to determine the final surface roughness for each sample.

Evaluation of microhardness

The Vickers microhardness of the specimens was evaluated using a diamond pyramid indenter applied to the material surface under a specified load for a fixed duration. In the present study, a Shimadzu HMV-G31DT microhardness tester was used, with a load of 2.942 N (HV0.3) applied for 20 seconds. The Vickers hardness number (VHN) was calculated by measuring the dimensions of the indentation formed on the specimen surface.

Evaluation of compressive strength

Cylindrical specimens measuring 4 mm in diameter and 6 mm in height were fabricated using stainless steel split molds in accordance with ISO 9917-1:2007 standards. To facilitate easy removal of the specimens, a thin layer of cocoa butter was applied to the inner surfaces of the molds. The prepared material was placed into the molds and covered with polyester strips and glass slides, followed by gentle pressure to eliminate entrapped air and obtain a smooth surface. After 30 minutes, the molds were carefully removed, and the specimens were stored in distilled water at 37 °C for 24 hours for conditioning. Subsequently, compressive strength testing was performed using a universal testing machine (Instron Electro Plus® E3000). A compressive load was applied along the longitudinal axis of each specimen at a crosshead speed of 1 mm/min until fracture occurred, and the compressive strength values were recorded in megapascals (MPa).

Statistical analysis

Data were analyzed using SPSS software version 23.0. The numerical results were expressed as mean ± standard deviation (SD), assuming a normal distribution of data. One-way analysis of variance (ANOVA) was performed to assess overall differences among the groups, followed by Tukey's honestly significant difference (HSD) post hoc test for pairwise comparisons. A p-value of ≤ 0.05 was considered statistically significant.

Results and Discussion

FTIR

The FTIR spectra of the modified glass ionomer cements are shown in **Figures 2 part a and b**. In titanium nanoparticles–modified GIC **(Figure 2a)**, a band around 560–580 cm^{-1}

corresponds to Ti–O–Ti stretching vibrations, confirming the presence of titanium nanoparticles. A prominent peak near ~1020–1050 cm^{-1} represents Si–O/P–O asymmetric stretching of the glass ionomer matrix, while bands at ~1450 cm^{-1} and ~1620 cm^{-1} correspond to C–O and carboxylate (COO^-) vibrations, respectively. Broad bands near ~2900 cm^{-1} and ~3300–3400 cm^{-1} indicate C–H and O–H stretching vibrations **(Figure 2a)**. Similarly, the spectrum of chitosan-modified GIC **(Figure 2b)** showed peaks around ~1020–1050 cm^{-1} corresponding to P–O/Si–O stretching, while bands near ~1450 cm^{-1} and ~1620–1650 cm^{-1} represent C–O and amide (C=O/N–H) vibrations characteristic of chitosan. The broad band around ~3300–3400 cm^{-1} corresponds to O–H and N–H stretching vibrations. These findings confirm the successful incorporation of titanium nanoparticles and chitosan into the GIC matrix **(Figure 2b)**.

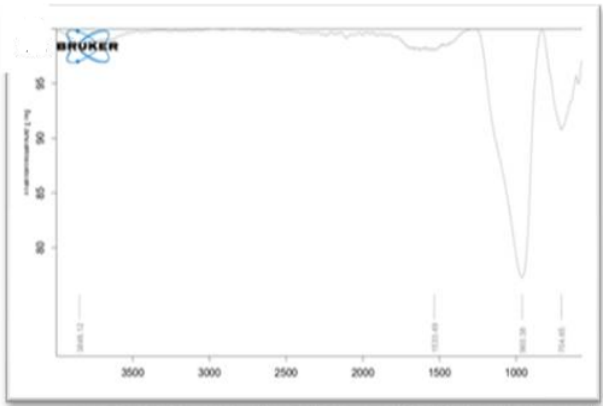

a)

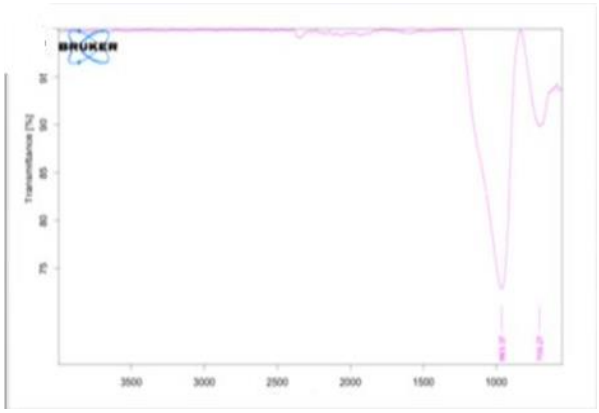

b)

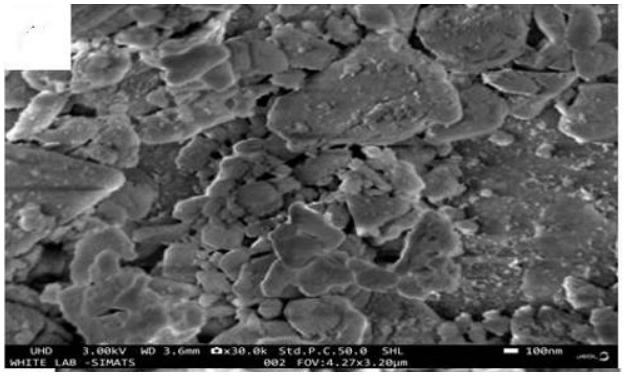

c)

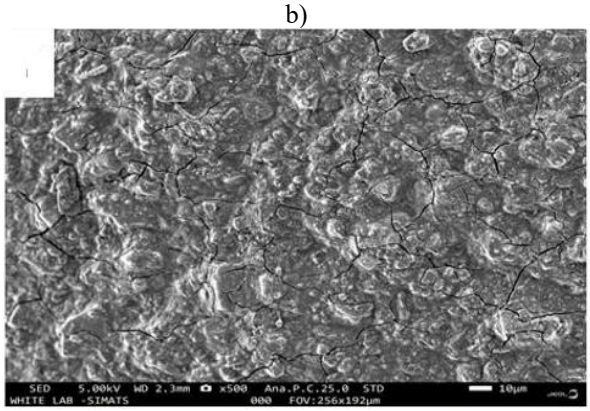

d)

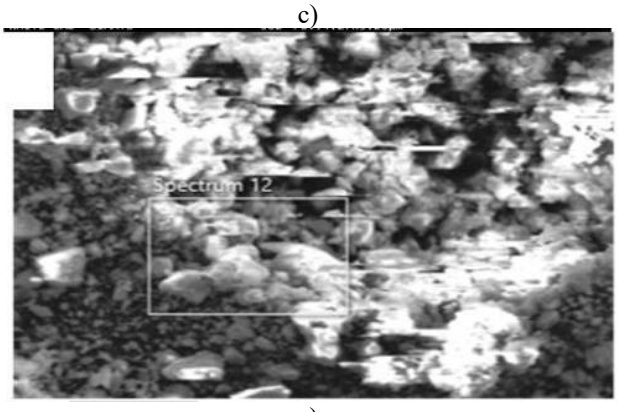

e)

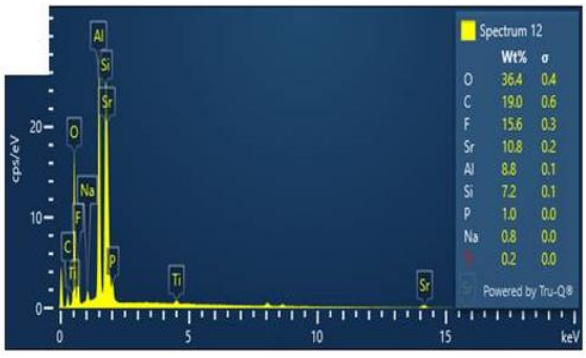

f)

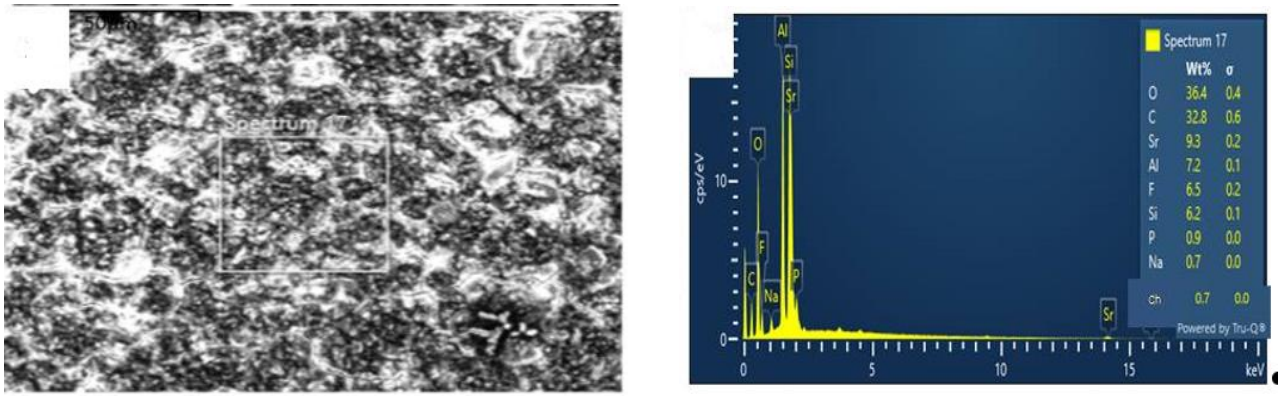

g) h)

Figure 2. Characterization of titanium- and chitosan-modified glass ionomer cement.
a) FTIR spectrum of titanium nanoparticle–modified GIC showing characteristic functional groups. b) FTIR spectrum of chitosan nanoparticle–modified GIC. c) SEM micrograph of titanium nanoparticles showing agglomerated nanostructures. d) SEM micrograph of chitosan nanoparticles exhibiting relatively homogeneous morphology. e) SEM image indicating the region selected for elemental analysis in titanium-modified GIC. f) EDX spectrum confirming the elemental composition and presence of titanium. g) SEM image showing the selected region for elemental analysis in chitosan-modified GIC. h) EDX spectrum demonstrating the elemental composition of the modified matrix.

SEM

The SEM micrographs of the modified glass ionomer cements showed noticeable changes in surface morphology after nanoparticle incorporation. The titanium nanoparticle–modified GIC exhibited a relatively dense and compact microstructure with uniformly distributed particles within the glass matrix, suggesting good nanoparticle dispersion **(Figure 2c)**. In contrast, the chitosan-modified GIC showed a slightly heterogeneous structure with irregular particle distribution and clustered regions. These observations indicate the successful incorporation of titanium nanoparticles and chitosan into the GIC matrix, which may contribute to improved material properties **(Figure 2d)**.

EDX

The EDX spectra of the modified glass ionomer cements revealed the presence of several elements characteristic of the GIC matrix, including oxygen (O), carbon (C), strontium (Sr), aluminum (Al), fluorine (F), silicon (Si), phosphorus (P), and sodium (Na). In both groups, oxygen was the most abundant element, comprising approximately 36.4 wt%. In the titanium nanoparticle-modified GIC, the elemental composition showed carbon (19.0 wt%), fluorine (15.6 wt%), strontium (10.8 wt%), aluminum (8.8 wt%), and silicon (7.2 wt%), along with trace elements such as sodium (0.8 wt%) and titanium (0.2 wt%). The detection of titanium in the EDX spectrum confirms the successful incorporation of titanium nanoparticles within the glass ionomer cement matrix **(Figures 2e and 2f)**. In the chitosan-modified GIC, carbon was present at 32.8 wt%, followed by strontium (9.3 wt%), aluminum (7.2 wt%), fluorine (6.5 wt%), and silicon (6.2 wt%), while minor elements such as phosphorus (0.9 wt%), sodium (0.7 wt%), and chitosan (0.7 wt%) were also detected **(Figures 2g and 2h)**.

Antibacterial activity

The antimicrobial evaluation of the experimental materials demonstrated significant differences among the tested groups against *Streptococcus mutans* and *Lactobacillus acidophilus*. The 5% green-mediated chitosan nanoparticle–modified GIC exhibited the largest zones of inhibition, measuring 19.37 ± 1.24 mm against *S. mutans* and 18.41 ± 1.19 mm against *L. acidophilus*, followed by the titanium nanoparticle–modified GIC, which showed inhibition zones of 14.52 ± 1.08 mm and 13.64 ± 1.12 mm, respectively. In contrast, conventional GIC demonstrated the lowest antibacterial activity, with inhibition zones of 9.76 ± 0.95 mm against *S. mutans* and 8.84 ± 0.88 mm against *L. acidophilus* **(Table 1)**. Further statistical evaluation using Tukey's post-hoc multiple comparison test confirmed significant differences between the experimental groups. The mean difference between chitosan-modified GIC and titanium-modified GIC was 4.81 mm ($p = 0.003$), while the difference between chitosan-modified GIC and conventional GIC was 9.59 mm ($p < 0.001$). Similarly, a significant difference was observed between titanium-modified GIC and conventional GIC (mean difference = 4.78 mm, $p = 0.007$), indicating that the incorporation of nanoparticles significantly enhances the antimicrobial performance of glass ionomer cement **(Table 2)**. The minimum inhibitory concentration (MIC) analysis further supported these findings, where chitosan nanoparticle–modified GIC demonstrated the lowest MIC values, measuring 21.8 ± 2.4 µg/mL against *S. mutans* and 25.6 ± 2.7 µg/mL against *L. acidophilus*. The titanium nanoparticle–modified GIC exhibited intermediate MIC values of 42.6 ± 3.1 µg/mL and 48.3 ± 3.6 µg/mL, respectively, whereas conventional GIC showed the highest MIC values, measuring 68.9 ± 4.2 µg/mL against *S. mutans* and 74.5 ± 4.8 µg/mL against *L. acidophilus* **(Table 3)**. Lower MIC values indicate greater antimicrobial efficacy, highlighting the superior inhibitory capability of chitosan-modified GIC against cariogenic bacteria.

Table 1. Mean Zone of Inhibition (mm) of titanium- and Chitosan-Modified Glass Ionomer Cement Against *Streptococcus mutans and Lactobacillus acidophilus*

Group	Green-mediated NP-modified GIC	*Streptococcus mutans*(mm) Mean ± SD	*Lactobacillus acidophilus* (mm) Mean ± SD	Overall Mean ± SD (mm)	F value	P value
Group I	5% TiO_2-GIC	14.52 ± 1.08	13.64 ± 1.12	14.08 ± 1.10		
Group II	5% Chi-GIC	19.37 ± 1.24	18.41 ± 1.19	18.89 ± 1.21	52.73	0.0004
Group III	**Conventional**	**9.76 ± 0.95**	**8.84 ± 0.88**	**9.30 ± 0.91**		

Values are expressed as mean ± standard deviation (SD). Larger zones of inhibition indicate greater antimicrobial activity. Statistical analysis was performed using one-way analysis of variance (ANOVA) followed by Tukey's post-hoc test for pairwise comparisons. A p-value < 0.05 was considered statistically significant.

Table 2. Post-hoc Tukey Multiple Comparison of Antimicrobial Activity Among Groups

Comparison Groups	Mean difference (mm)	Std. Error	95% CI (Lower–Upper)	p-value
Group I vs Group II	4.81	1.21	1.92 – 7.70	0.003
Group II vs Group III	9.59	1.34	6.34 – 12.84	<0.001
Group I vs Group III	**4.78**	**1.15**	**2.01 – 7.55**	**0.007**

Pairwise comparisons between experimental groups were performed using Tukey's post-hoc test following one-way ANOVA. p < 0.05 indicates a statistically significant difference between groups.

Table 3. Minimum Inhibitory Concentration (MIC) of Titanium- and Chitosan-Modified Glass Ionomer Cement Against Oral Cariogenic Bacteria (µg/mL)

Group	Green-mediated NP-modified GIC	*S.mutans* Mean ± SD	*L.acidophilus* Mean ± SD	Overall Mean ± SD	P value
Group I	5% TiO_2-GIC	42.6 ± 3.1	48.3 ± 3.6	45.4 ± 3.4	
Group II	5% Chi-GIC	21.8 ± 2.4	25.6 ± 2.7	23.7 ± 2.5	0.0006
Group III	Conventional GIC	68.9 ± 4.2	74.5 ± 4.8	71.7 ± 4.5	

Values are presented as mean ± standard deviation (SD). Lower MIC values indicate greater antimicrobial efficacy. Statistical analysis was performed using one-way ANOVA, with an overall p-value = 0.0006, indicating significant differences among the groups (p < 0.05).

Surface roughness

The surface roughness analysis demonstrated a significant difference among the tested groups. The 5% green-mediated titanium nanoparticle–modified GIC exhibited the lowest surface roughness (0.82 ± 0.07 µm), followed by the chitosan nanoparticle–modified GIC (0.94 ± 0.08 µm), while the conventional GIC showed the highest roughness (1.18 ± 0.10 µm) **(Table 4)**. Statistical analysis using one-way ANOVA revealed a significant difference among the groups (p = 0.004). The smoother surface observed in the titanium-modified group may be attributed to the nano-sized particles filling microvoids within the glass ionomer matrix, resulting in a more compact and homogeneous structure **(Figure 3a)**. The chitosan-modified GIC also exhibited reduced roughness compared with conventional GIC, which may be related to improved matrix cohesion due to interactions between chitosan and the polyacrylic acid component of the cement **(Figure 3b)**. In contrast, the higher roughness observed in conventional GIC may be associated with the presence of larger filler particles and inherent surface irregularities of the unmodified material. Overall, these findings suggest that nanoparticle incorporation, particularly titanium nanoparticles, can improve the surface characteristics of glass ionomer cement, which may help reduce bacterial adhesion and plaque accumulation in clinical applications.

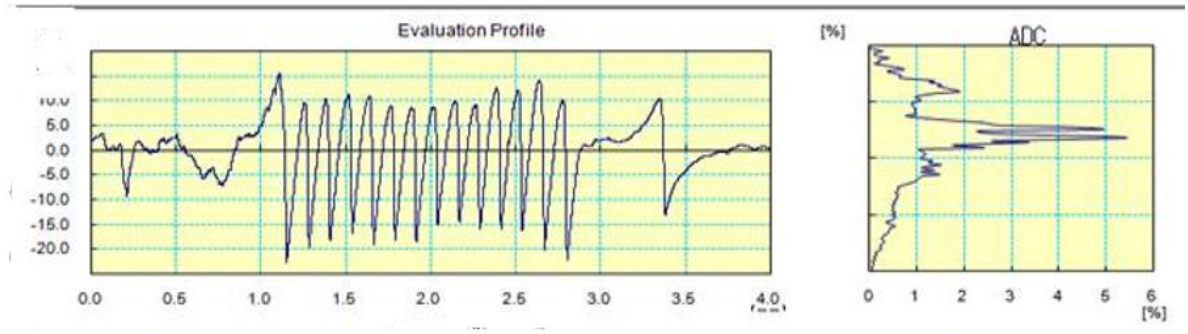
Evaluation Profile
10.0
5.0
0.0
-5.0
-10.0
-15.0
-20.0
0.0 0.5 1.0 1.5 2.0 2.5 3.0 3.5 4.0
[%]
ADC
0 1 2 3 4 5 6
[%]

a)

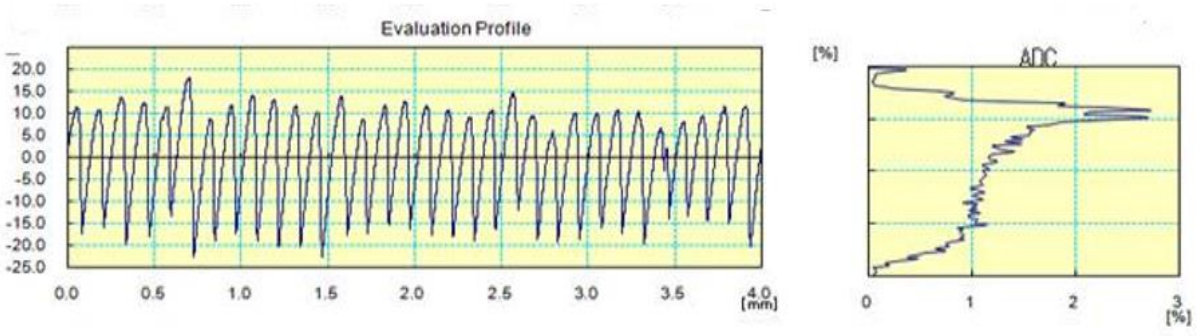
Evaluation Profile
20.0
15.0
10.0
5.0
0.0
-5.0
-10.0
-15.0
-20.0
-25.0
0.0 0.5 1.0 1.5 2.0 2.5 3.0 3.5 4.0
[mm]
[%]
ADC
0 1 2 3
[%]

b)

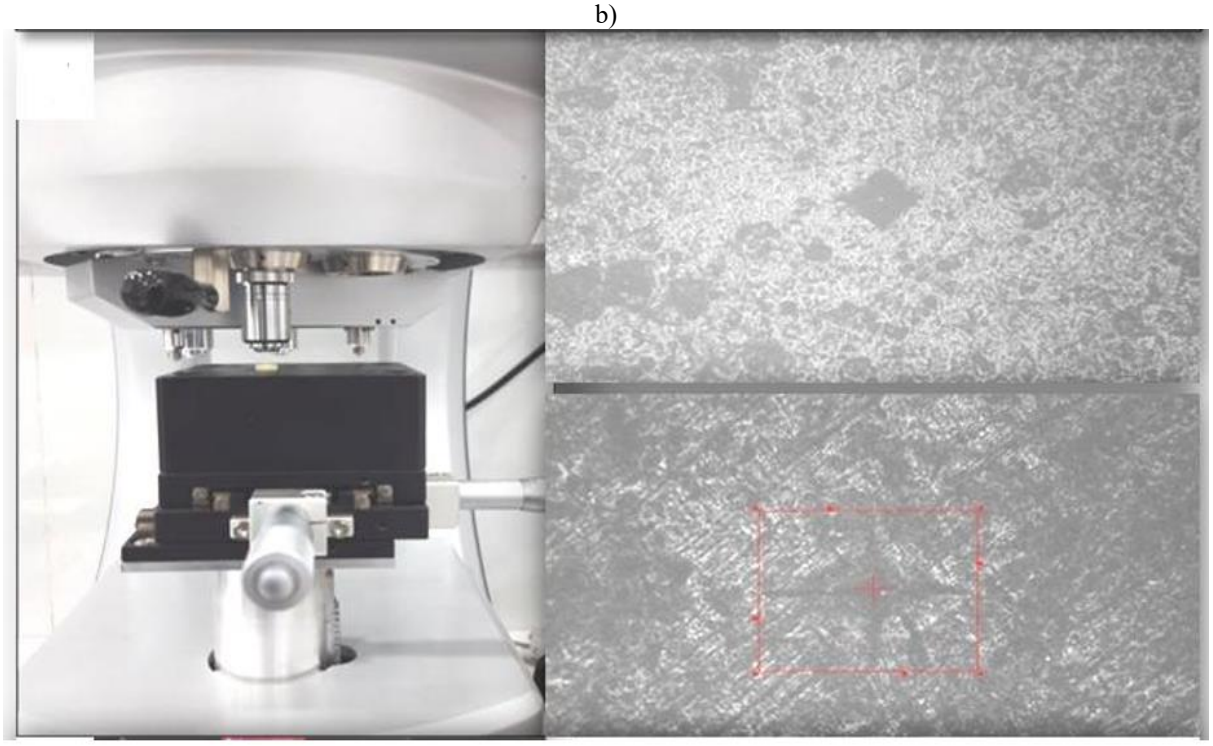

c)

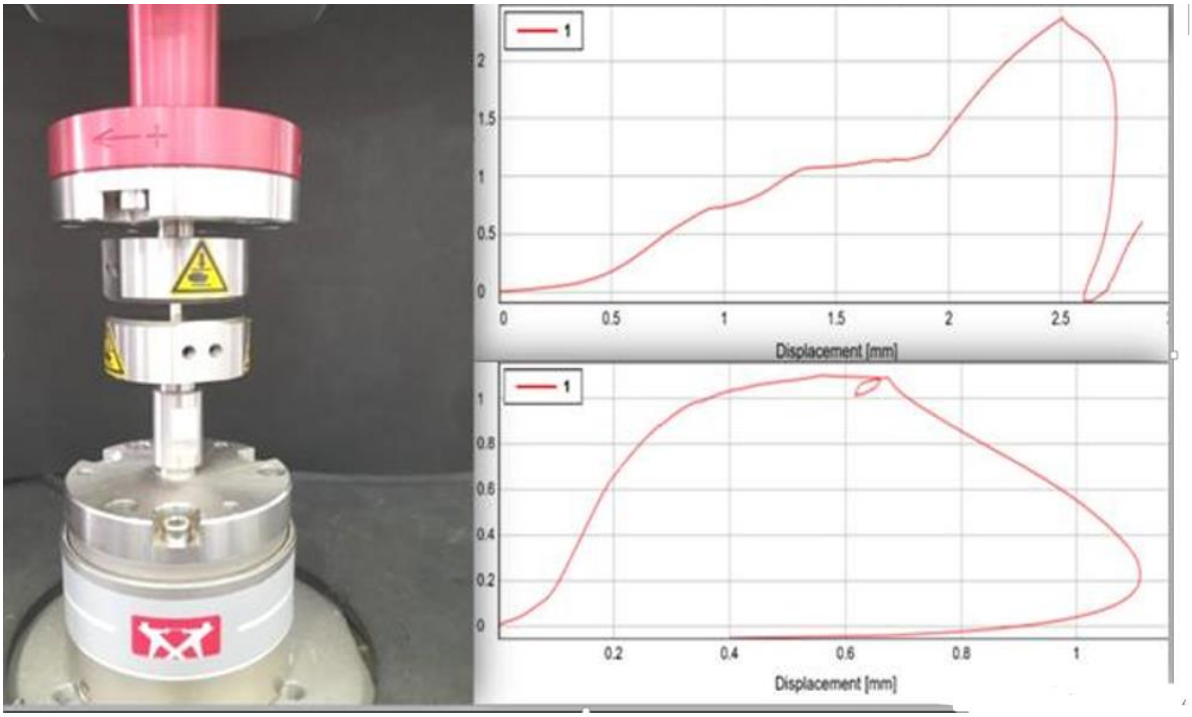

d)

Figure 3. Evaluation of surface and mechanical properties of nanoparticle-modified glass ionomer cement. a) Surface roughness profile of titanium nanoparticle–modified glass ionomer cement obtained using a surface profilometer, showing surface topography used for roughness calculation. b) Surface roughness profile of chitosan nanoparticle–modified glass ionomer cement showing the corresponding profilometric evaluation curve. c) Vickers microhardness testing with representative indentation micrographs; the upper image represents titanium nanoparticle–modified GIC, while the lower image represents chitosan nanoparticle–modified GIC. d) Compressive strength testing using a universal testing machine (UTM) with corresponding load–displacement curves for titanium and chitosan nanoparticle–modified glass ionomer cement specimens.

Microhardness

The Vickers microhardness results demonstrated a significant difference among the tested groups. The 5% green-mediated titanium nanoparticle–modified GIC exhibited the highest microhardness value (78.42 ± 3.15 VHN), followed by the chitosan nanoparticle–modified GIC (69.87 ± 2.94 VHN), while the conventional GIC showed the lowest microhardness (61.35 ± 2.48 VHN) **(Table 4)**. Statistical analysis using one-way ANOVA revealed a significant difference among the groups ($p = 0.002$). The improved hardness observed in the titanium-modified group may be attributed to the reinforcing effect and high mechanical strength of titanium nanoparticles, which enhance the structural integrity of the GIC matrix **(Figure 3c)**.

Compressive strength

The compressive strength values of the tested materials are presented in **Table 4**. The 5% green-mediated titanium nanoparticle–modified GIC exhibited the highest compressive strength (165.42 ± 8.36 MPa) among the groups. This was followed by the chitosan nanoparticle–modified GIC, which showed a compressive strength of 148.27 ± 7.92 MPa **(Figure 3d)**. In contrast, the conventional GIC demonstrated the lowest compressive strength (129.58 ± 6.84 MPa). Statistical analysis using one-way ANOVA revealed a significant difference among the groups ($p = 0.001$).

Table 4. Surface Roughness (Ra), Vickers Microhardness, and Compressive Strength of Titanium- and Chitosan-Modified Glass Ionomer Cement

Parameter	Group	Green-mediated NP-modified GIC	Mean ± SD	p-value
Surface roughness (Ra, µm)	Group I	5% TiO_2-GIC	0.82 ± 0.07	0.004
	Group II	5% Chi-GIC	0.94 ± 0.08	
	Group III	Conventional GIC	1.18 ± 0.10	

Vickers Microhardness (VHN)	Group I	5% TiO_2-GIC	78.42 ± 3.15	0.002
	Group II	5% Chi-GIC	69.87 ± 2.94	
	Group III	Conventional GIC	61.35 ± 2.48	
Compressive Strength (MPa)	Group I	5% TiO_2-GIC	165.42 ± 8.36	0.001
	Group II	5% Chi-GIC	148.27 ± 7.92	
	Group III	Conventional GIC	129.58 ± 6.84	

Values are expressed as mean ± standard deviation (SD). Surface roughness was measured using a profilometer, and the average roughness value (Ra) was recorded in micrometers (µm). Microhardness was measured using a Vickers microhardness tester under a load of 2.942 N (HV0.3) applied for 20 seconds. Compressive strength was measured using a universal testing machine with load applied along the longitudinal axis at a crosshead speed of 1 mm/min until specimen failure. Results are presented in megapascals (MPa). Statistical analysis was performed using one-way analysis of variance (ANOVA) to compare the groups, with $p < 0.05$ considered statistically significant

Glass ionomer cement (GIC) continues to play a pivotal role in restorative dentistry because of its inherent advantages, such as chemical adhesion to tooth structure, fluoride release, and favorable biocompatibility. Despite these benefits, the relatively low mechanical strength and susceptibility to surface degradation restrict its application in stress-bearing restorations, thereby necessitating continuous material optimization and reinforcement strategies [5]. In recent years, nanotechnology has emerged as a promising approach for improving the physical and biological properties of restorative materials. Furthermore, the incorporation of nanoparticles synthesized through green chemistry routes has gained increasing attention due to their enhanced biocompatibility, environmental sustainability, and potential synergistic biological activity [32, 33]. Therefore, the present study employed a green nanotechnology-based approach to modify conventional GIC using Neem-mediated titanium dioxide (TiO_2) nanoparticles and Eucalyptus-enhanced chitosan nanoparticles. The results demonstrated that such bio-modifications significantly improved the antimicrobial efficacy, mechanical strength, and surface characteristics of conventional GIC, suggesting their potential for enhancing the clinical performance of restorative materials.

An important aspect of the present investigation was the adoption of plant-mediated green synthesis for nanoparticle preparation. Green synthesis methods have gained increasing importance in biomaterials research because of their environmentally sustainable nature and the ability of plant-derived phytochemicals to function as natural reducing and stabilizing agents during nanoparticle formation. In the present study, Neem extract was utilized for the synthesis of titanium dioxide nanoparticles, while Eucalyptus extract was used to enhance chitosan nanoparticle preparation. These plant extracts contain bioactive compounds such as flavonoids, phenolic acids, and terpenoids that facilitate nanoparticle stabilization and prevent aggregation, thereby promoting uniform dispersion within the glass ionomer matrix.The use of phytochemical-assisted nanoparticle synthesis may also contribute to the enhanced biological activity observed in the present study [34-39]. Phytochemicals present in Neem extract—including nimbidin, nimbin, nimbolide, azadirachtin, gallic acid, epicatechin, catechin, and margolone—are known to possess antimicrobial properties [31]. The integration of these phytochemicals during nanoparticle synthesis may therefore create a synergistic interaction between nanoparticles and plant-derived bioactive molecules, potentially enhancing the antibacterial performance of the modified GIC.

Antibacterial properties of restorative materials are essential to prevent bacterial colonization at the tooth–restoration interface and reduce secondary caries. Oral bacteria, particularly *Streptococcus mutans*, are strongly associated with caries development, making antimicrobial incorporation important for improving restoration longevity [40]. In this study, nanoparticle-modified GICs showed significantly higher antibacterial activity than conventional GICs. Chitosan-modified GIC exhibited the highest activity, followed by TiO_2-modified GIC. The superior effect of chitosan is due to its polycationic nature, which interacts with negatively charged bacterial membranes, disrupting membrane integrity and causing cell death. The antibacterial activity of TiO_2-modified GIC is attributed to both titanium dioxide nanoparticles and neem-derived phytochemicals. Neem contains compounds such as nimbidin, nimbin, nimbolide, azadirachtin, gallic acid, epicatechin, catechin, and margolone with strong antimicrobial effects; azadirachtin is the primary bioactive component [31]. These findings are consistent with previous studies. Nadia Alaee *et al*. [41] reported enhanced antimicrobial activity with 3% TiO_2 GIC. P.S. *et al*. [42] observed moderate improvement, while Hamid N *et al*. [43] demonstrated increased compressive strength and antibacterial activity against *S. mutans*. The antimicrobial mechanism of TiO_2 involves ROS generation (hydroxyl radicals and superoxide ions) via photocatalysis, leading to membrane damage, lipid peroxidation, DNA damage, and bacterial cell death [44].

Chitosan-modified GIC showed significantly greater antimicrobial activity than conventional GIC, mainly due to the intrinsic antibacterial properties of chitosan nanoparticles. Its polycationic structure enables electrostatic interaction with negatively charged bacterial membranes, disrupting integrity, increasing permeability, and causing leakage of intracellular components, leading to cell death [45]. Chitosan also chelates essential metal ions and inhibits microbial enzymes. Its nanoscale size enhances surface interaction, improving inhibition of *Streptococcus mutans*. Eucalyptus extract used in synthesis may further enhance

this effect. It contains bioactive compounds such as eucalyptol, flavonoids, tannins, phenolic acids, terpenoids, and α-pinene with known antimicrobial activity [45]. These disrupt membranes and inhibit microbial metabolism, showing a synergistic effect with chitosan nanoparticles. Previous studies also report improved antimicrobial and mechanical properties of chitosan-modified GIC [46, 47]. TiO_2 nanoparticles have been widely studied as reinforcing fillers in dental materials [48, 49], and Thomas *et al*. (2014) demonstrated their antibacterial effect against oral bacteria [50]. Their mechanism involves reactive oxygen species generation and metabolic interference. In contrast, conventional GIC shows lower antibacterial activity, mainly due to limited fluoride release. Overall, incorporation of bioactive nanoparticles, especially chitosan, significantly enhances the antimicrobial potential of GIC and may help reduce bacterial colonization and secondary caries.

Surface roughness is a critical factor influencing plaque accumulation, bacterial adhesion, and long-term restoration performance. Surface microhardness plays a crucial role in determining the wear resistance and long-term durability of restorative materials. Rough restorative surfaces facilitate microbial colonization and increase the risk of secondary caries and periodontal complications [51, 52]. Therefore, restorative materials with smoother surfaces are clinically desirable. In the present study, TiO_2-modified GIC exhibited the lowest surface roughness among the tested materials. The improved surface characteristics may be attributed to the nanoscale dimensions of titanium dioxide particles, which allow them to fill microscopic voids within the glass ionomer matrix. This results in a more compact and homogeneous structure with fewer surface irregularities.Another contributing factor may be the formation of stable complexes between TiO_2 nanoparticles and the polyacrylic acid matrix, which enhances colloidal stability and prevents nanoparticle agglomeration [53, 54]. The improved particle–matrix interaction and reduced surface irregularities may ultimately help reduce bacterial adhesion and plaque accumulation on restorative surfaces. Although TiO_2 nanoparticles demonstrated superior mechanical reinforcement, chitosan-modified GIC also exhibited significant improvements compared with conventional GIC. Chitosan nanoparticles are known to reduce the interfacial surface tension between components within the glass ionomer matrix, thereby improving internal cohesion and structural stability. Due to their nanoscale size, chitosan particles possess a high surface area and charge density, which facilitates stronger interaction with the surrounding matrix environment [55, 56].

In the present study, TiO_2-modified GIC demonstrated significantly higher microhardness compared with chitosan-modified and conventional GIC.The improved microhardness can be attributed to the dense packing of nanoparticles within the cement structure, which enhances the rigidity of the matrix and reduces surface deformation under applied loads. The nanoscale size of the particles increases the surface area available for interaction with the polyacrylic acid matrix, thereby improving interfacial bonding and structural stability.These findings are consistent with previous studies. Fathi *et al*. [57] reported significant improvements in microhardness following the incorporation of 3% and 5% CA-TiO_2 nanoparticles into GIC. Similarly, Garcia-Contreras *et al*. [53] observed a significant increase in microhardness when TiO_2 nanoparticles were incorporated into restorative GIC formulations. Abozaid D *et al*. also reported that the addition of 10% CA-TiO_2 nanoparticles resulted in the highest microhardness values [5]. Researchers [58] reported that the addition of chitosan positively influenced the microhardness values of GIC. However, because chitosan is a polymeric biomaterial rather than a rigid metallic nanoparticle, its reinforcing capacity is comparatively lower than that of TiO_2 nanoparticles. Nevertheless, the statistically significant improvement observed compared with conventional GIC indicates its clinical relevance, particularly in minimally invasive restorative procedures. Similar observations were reported by Tuzuner and Ulusu [59]. Thus, the chitosan-modified GIC demonstrated moderate improvement in hardness, likely due to interactions between chitosan and the polyacrylic acid matrix that enhance matrix cohesion. These findings indicate that nanoparticle incorporation can improve the mechanical properties of glass ionomer cement, particularly with titanium nanoparticles.

Mechanical strength is a critical determinant of the long-term clinical performance of restorative materials. In the present study, Neem-mediated TiO_2-modified GIC demonstrated the highest compressive strength among the evaluated groups. This improvement can be attributed to the intrinsic mechanical strength and high stiffness of titanium dioxide nanoparticles and their ability to function as reinforcing fillers within the glass ionomer matrix. The incorporation of nanoparticles within the GIC matrix promotes uniform stress distribution and reduces crack propagation by reinforcing the matrix–filler interface. TiO_2 nanoparticles act as load-bearing structures that enhance the structural integrity of the material under compressive forces. Furthermore, the green synthesis process using Neem extract may improve nanoparticle dispersion and stability within the matrix, thereby maximizing their reinforcing potential. Another important factor contributing to the increased compressive strength is the nanoscale size of TiO_2 particles, which enables them to occupy voids between larger glass particles in the GIC powder. This results in denser particle packing and improved bonding with the polyacrylic acid matrix [60, 61]. Consequently, nanoparticles function as secondary fillers between GIC powder particles and strengthen the overall cement structure [62, 63]. Similar improvements in compressive strength have been reported by Elsaka SE *et al*. following the incorporation of TiO_2 nanoparticles into GIC formulations [64]. These findings indicate that the incorporation of nanoparticles, particularly titanium nanoparticles, significantly enhances the compressive strength of glass

ionomer cement compared with the unmodified material.

When the findings of all evaluated parameters are collectively considered, a clear synergistic effect of nanoparticle incorporation on GIC performance becomes evident. TiO_2 nanoparticles primarily contributed to mechanical reinforcement and surface stabilization due to their high stiffness and nanoscale filler characteristics. In contrast, chitosan nanoparticles contributed more prominently to biological performance through their inherent antimicrobial properties and electrostatic interactions with bacterial cells. The integration of green synthesis with nanoparticle reinforcement, therefore, provides a dual advantage by simultaneously improving mechanical durability and antibacterial efficacy. Such multifunctional enhancements are particularly desirable in restorative materials because they address two major clinical limitations associated with conventional GIC: insufficient mechanical strength and susceptibility to bacterial colonization. The improved compressive strength, microhardness, surface smoothness, and antibacterial performance observed in the present study suggest that green-synthesized nanoparticle-modified GIC may significantly expand the clinical applicability of conventional GIC. Neem-mediated TiO_2-modified GIC may be particularly suitable for stress-bearing restorations and posterior applications. In contrast, chitosan-modified GIC may serve as a biologically favorable restorative material in patients with high caries risk. However, since the present investigation was conducted under invitro conditions, further studies incorporating aging protocols, thermal cycling, and long-term invivo evaluation are necessary to validate the clinical durability and performance of these modified restorative materials.

Conclusion

The incorporation of green-mediated nanoparticles significantly improved the biological and mechanical performance of glass ionomer cement. Chitosan nanoparticle–modified GIC demonstrated superior antibacterial activity against *Streptococcus mutans* and *Lactobacillus acidophilus*, indicating enhanced potential for inhibiting cariogenic bacteria. In contrast, titanium nanoparticle–modified GIC exhibited improved mechanical characteristics, including higher microhardness, lower surface roughness, and greater compressive strength compared with conventional GIC. These findings highlight that nanoparticle modification, particularly with chitosan and titanium, can effectively enhance the antimicrobial efficacy, mechanical strength, and surface properties of glass ionomer cement, suggesting its promising role in improving restorative material performance and reducing the risk of secondary caries in clinical dentistry.

Acknowledgments: None

Conflict of interest: None

Financial support: None

Ethics statement: The study protocol was approved by Institutional Ethics Committee, Saveetha Dental College and Hospitals, Chennai, India.

References

1. Najeeb S, Khurshid Z, Zafar MS, Khan AS, Zohaib S, Martí JM, et al. Modifications in glass ionomer cements: nano-sized fillers and bioactive nanoceramics. Int J Mol Sci. 2016;17(7):1134. doi:10.3390/ijms17071134
2. Sheshadri A, Kittiskulnam P, Johansen KL. Investigating the effects of physical activity on the amount of muscle cramp pain in hemodialysis patients. J Integr Nurs Palliat Care. 2024;5:8–13. doi:10.51847/wZhaI3rJNj
3. Sheshadri A, Valeh EAA. Patients' preferences for addressing spirituality during hospitalization: a cross-sectional study from a Lebanese tertiary care center. J Integr Nurs Palliat Care. 2025;6:83–94. doi:10.51847/TIVZLzKeLc
4. Mustafa HA, Soares AP, Paris S, Elhennawy K, Zaslansky P. The forgotten merits of GIC restorations: a systematic review. Clin Oral Investig. 2020;24(7):2189–201. doi:10.1007/s00784-020-03334-0
5. Abozaid D, Ayad A, Ibrahim Y, Azab A, El-Aal MA, El-Safty S. Green-synthesized titanium dioxide nanoparticle-modified glass ionomer cement: in vitro and in silico assessment of mechanical, physical, and safety properties performance. Sci Rep. 2026;16(1):5890. doi:10.1038/s41598-026-37048-2
6. Abdelwahab FH, Abd-Allah SMM, Omar HSA, Elhadary AEMAE, Ahmad MM. Evaluating the effects of plasma irradiation and stevia on gene expression and immune responses in HepG2 cells. Asian J Curr Res Clin Cancer. 2025;5(1):20–9. doi:10.51847/HBLDVGjDM4
7. Al-Balushi Z, Al-Hajri M, Khalfan O. Time-dependent prognostic value of Ki-67 in early breast cancer: validation of visual and hot-spot scoring methods. Asian J Curr Res Clin Cancer. 2025;5(1):42–58. doi:10.51847/bucirz2PEE
8. Low LF, Islahudin F, Saffian SM. Formulation of a written counseling resource for COVID-19 patients undergoing subcutaneous anticoagulant treatment. Ann Pharm Pract Pharmacother. 2024;4:65–72. doi:10.51847/jnYzmx6Dak
9. Hao C, Yang L, Mei W. Updated review on the phytochemicals and pharmacological properties of Ipomoea batatas L. Ann Pharm Pract Pharmacother. 2025;5:151–63. doi:10.51847/blnjilB2ZO
10. Lv X, Yang L, Fan Z, Bao X. Synthesis and biological assessment of novel quinazolinone–piperazine hybrid derivatives as antimicrobial agents. Pharm Sci Drug Des. 2024;4:16–25. doi:10.51847/OCT1Q8Fm7d

11. Martin C, Wright B, Scott O. Synthesis, structural characterization, DFT studies, and anticancer activity of benzimidazole-derived imines with Cu (II) and Co (III) complexes. Pharm Sci Drug Des. 2025;5:297–314. doi:10.51847/jRpfxAeueC
12. Anzano A, Ammar M, Papaianni M, Grauso L, Sabbah M, Capparelli R, et al. Physicochemical characterization and in vitro anti-obesity potential of Anethum graveolens (dill) seed cake. Spec J Pharmacogn Phytochem Biotechnol. 2024;4:39–48. doi:10.51847/uNSbIYlQor
13. Tanaka A, Mori Y, Sakamoto H, Fujii K. Larvicidal potential of essential oils from Ethiopian medicinal plants against Anisakis L3 larvae: chemical composition and cytotoxic evaluation. Spec J Pharmacogn Phytochem Biotechnol. 2025;5:253–62. doi:10.51847/Y2ND34xN4K
14. Wylie MR, Merrell DS. The antimicrobial potential of the neem tree, Azadirachta indica. Front Pharmacol. 2022;13:891535. doi:10.3389/fphar.2022.891535
15. Chava VR, Manjunath SM, Rajanikanth AV, Sridevi N. The efficacy of neem extract on four microorganisms responsible for causing dental caries: an in vitro study. J Contemp Dent Pract. 2012;13:769–72. doi:10.5005/jp-journals-10024-1227
16. Soygun K, Soygun A, Dogan MC. The effects of chitosan addition to glass ionomer cement on microhardness and surface roughness. J Appl Biomater Funct Mater. 2021;19. doi:10.1177/2280800021989706
17. Petri DF, Donega J, Benassi AM, Bocangel JA. Preliminary study on chitosan-modified glass ionomer restoratives. Dent Mater. 2007;23(8):1004–10. doi:10.1016/j.dental.2006.06.038
18. O'Connor D, Walsh P, Murphy B. Evaluation of methanolic extracts from six ethnomedicinal plants for antibacterial efficacy and bioactive constituents. Interdiscip Res Med Sci Spec. 2024;4(1):144–53. doi:10.51847/zbJZnYvzjS
19. Zar H, Moore DP, Andronikou S, Argent AC, Avenant T, Cohen C, et al. Principles of diagnosis and treatment in children with acute pneumonia. Interdiscip Res Med Sci Spec. 2024;4(2):24–32. doi:10.51847/4RVz1Zxy4h
20. Rizzi FL, Romano LF, Farouk AS. Early-life establishment of the infant oral microbiome: a 15-month longitudinal study of microbial succession and mother-to-infant transmission patterns. J Curr Res Oral Surg. 2024;4:72–85. doi:10.51847/NpV9lui2oj
21. Weber JK, El Sherif AK, Romano LF. Capsule-conjugate vaccination against Porphyromonas gingivalis confers protection in a preclinical model of periodontal bone loss. J Curr Res Oral Surg. 2025;5:105–18. doi:10.51847/v8fDF8v9PY
22. Delcea C, Gyorgy M, Siserman C, Popa-Nedelcu R. Impact of maladaptive cognitive schemas on suicidal behavior in adolescents during the COVID-19 pandemic: a predictive study. Int J Soc Psychol Asp Healthc. 2024;4:42–6. doi:10.51847/EHCf9HzLEP
23. Brooks HS, Allen TJ, Foster RM. Attitudes toward mandatory COVID-19 vaccination policies in Alberta: evidence from Reddit during the fourth wave. Int J Soc Psychol Asp Healthc. 2024;4:138–46. doi:10.51847/m3Pr7zrNn3
24. Mazur K, Kaczmarek PD, Nowicka A. Cognitive processes and decision-making strategies of pharmacy students in antimicrobial stewardship cases. Ann Pharm Educ Saf Public Health Advoc. 2024;4:155–64. doi:10.51847/k5hvzOODJf
25. Hassan AR, Farouk SI, Abdelrahman ON. Can virtual microbiology labs achieve comparable outcomes to traditional hands-on wetlabs in pharmacy education? Ann Pharm Educ Saf Public Health Advoc. 2025;5:119–28. doi:10.51847/D55RlfgU0q
26. Hart OB, Reed CJ. Anti-neuroinflammatory effects of 50% ethanolic Curcuma longa extract in LPS-stimulated BV2 microglia. J Med Sci Interdiscip Res. 2025;5(1):1–12. doi:10.51847/bMiGiIU1tk
27. Peterson SL, Rogers EK. Enhancing accuracy of SARS-CoV-2 point-of-care testing through proficiency testing. J Med Sci Interdiscip Res. 2025;5(1):67–79. doi:10.51847/o7GFl1Vzrn
28. Monteiro NF, Lima HMR, da Silva FL, Sousa FCA, da Silva WC, Reis LCM, et al. Activity of Eucalyptus globulus essential oil in the control of bacteria in the oral cavity. Res Soc Dev. 2021;10(14):e60101420387. doi:10.33448/rsd-v10i14.2009
29. Balhaddad AA, AlSheikh RN. Effect of eucalyptus oil on Streptococcus mutans and Enterococcus faecalis growth. BDJ Open. 2023;9(1):26. doi:10.1038/s41405-023-00154-8
30. Mohammed N. In vitro antimicrobial activity of leaves extracts of eucalyptus spathulata against Streptococcus mutans and Candida albicans. J Al-Rafidain Univ Coll Sci. 2014;1:183–94. doi:10.55562/jrucs.v33i1.308
31. Banavar Ravi S, Nirupad S, Chippagiri P, Pandurangappa R. Antibacterial effects of natural herbal extracts on Streptococcus mutans. Int J Dent. 2017;2017:4921614. doi:10.1155/2017/4921614
32. Karimov D, Rakhimova N. The impact of socially responsible human resource management on employee innovation performance. Ann Organ Cult Leadersh Extern Engagem J. 2024;5:132–46. doi:10.51847/xJBYUl9BqH
33. Joungtrakul J, Smith ID. Exploring the path from organizational justice to organizational citizenship behavior. Ann Organ Cult Leadersh Extern Engagem J. 2025;6:31–5. doi:10.51847/DBvez9u8O9
34. Clark WJ, Davies CR, Hall SP. CircAXIN1-encoded AXIN1-295aa activates Wnt/β-catenin signaling to drive gastric cancer progression. Arch Int J Cancer Allied Sci. 2025;5(2):138–58. doi:10.51847/fhyhFRrfxD
35. Carter E, Morris DJ, Lee H, Thompson R. CircDLG1 drives anti-PD-1 resistance and gastric cancer progression. Arch Int J Cancer Allied Sci. 2025;5(2):13–33. doi:10.51847/snq9DXS1f2

36. Wong M, Chen K. Characteristics of institutional ethics committees and SOP implementation. Asian J Ethics Health Med. 2025;5:141–9. doi:10.51847/Wjo21pNqrd
37. Mai NT, Anh TQ, Ha PT. Navigating ethical and logistical challenges in establishing a nationwide cohort study. Asian J Ethics Health Med. 2024;4:152–69. doi:10.51847/uikLJkZC8a
38. Makoae M, Mokhele T, Naidoo I, Sifunda S, Sewpaul R. The influence of COVID-19 on standard child immunisation practices in South Africa. Bull Pioneer Res Med Clin Sci. 2025;5(1):28–36. doi:10.51847/tJtNDImcXV
39. Espinoza S, Lagunas M, Claudia R, Lovell JL. Association between loneliness and cannabis consumption among older adults. Bull Pioneer Res Med Clin Sci. 2025;5(1):73–85. doi:10.51847/eyyc1dnSwa
40. Hafshejani TM, Zamanian A, Venugopal JR, Rezvani Z, Sefat F, Saeb MR, et al. Antibacterial glass-ionomer cement restorative materials: a critical review on the current status of extended release formulations. J Control Release. 2017;262:317–28. doi:10.1016/j.jconrel.2017.07.041
41. Alaee N, Kimyai S, Maleki DS, Sharifi S. Titanium dioxide nanoparticles-modified dental glass ionomer cement. Curr Nanomed. 2026;16. doi:10.2174/0124681873406710251126063518
42. P S, Ks H, S G, Jannu A, Kusugal P, Ruttonji Z. Biosynthesized TiO_2 nanoparticles to enhance glass ionomer cement. Cureus. 2025;17(12):e98281. doi:10.7759/cureus.98281
43. Hamid N, Telgi RL, Tirth A, Tandon V, Chandra S, Chaturvedi RK. Titanium dioxide nanoparticles enriched glass-ionomer cement. J Clin Pediatr Dent. 2019;43(1):42–5. doi:10.17796/1053-4625-43.1.8
44. Besinis A, De Peralta T, Handy RD. Antibacterial effects of nanoparticles on Streptococcus mutans. Nanotoxicology. 2014;8(1):1–16. doi:10.3109/17435390.2012.742935
45. Yilmaz Atay H. Antibacterial activity of chitosan-based systems. Funct Chitosan. 2020:457–89. doi:10.1007/978-981-15-0263-7_15
46. Vasudevan S, Paulraj J, Maiti S. Effects of thermocycling on nanomodified glass ionomer cement. Int J Clin Pediatr Dent. 2025;18(6):724–32. doi:10.5005/jp-journals-10005-3179
47. Sahu D, Mehta G, Bhatia D. Comparative evaluation of compressive strength of modified glass ionomer cements. Int J Adv Res. 2019;7(4):1414–21. doi:10.21474/IJAR01/8968
48. Wetzel B, Rosso P, Haupert F, Friedrich K. Epoxy nanocomposites—fracture and toughening mechanisms. Eng Fract Mech. 2006;73:2375–98. doi:10.1016/j.engfracmech.2006.05.018
49. Xia Y, Zhang F, Xie H, Gu N. Nanoparticle-reinforced resin-based dental composites. J Dent. 2008;36(6):450–5. doi:10.1016/j.jdent.2008.03.001
50. Thomas A, Raj MS, Venkataramana J. Antimicrobial activity of TiO_2 nanoparticles against dental plaque isolates. Int J Bioassays. 2014;3(6):3106–10.
51. da Silva RC, Zuanon AC. Surface roughness of glass ionomer cements. Braz Dent J. 2006;17(2):106–9. doi:10.1590/s0103-64402006000200004
52. Al Hatem O, Ontiveros JC, Belles DM, Gonzalez MD, van der Hoeven R. Surface roughness and microbial adhesion on restorative materials. Dentistry J. 2025;13(11):498. doi:10.3390/dj13110498
53. Garcia-Contreras R, Scougall-Vilchis RJ, Contreras-Bulnes R, Sakagami H, Morales-Luckie RA, Nakajima H. Mechanical, antibacterial, and bond strength properties of nano-titanium-enriched glass ionomer cement. J Appl Oral Sci. 2015;23:321–8. doi:10.1590/1678-775720140496
54. Kanehira K, Banzai T, Ogino C, Shimizu N, Kubota Y, Sonezaki S. Properties of TiO_2-polyacrylic acid dispersions. Colloids Surf B Biointerfaces. 2008;64(1):10–5. doi:10.1016/j.colsurfb.2007.12.018
55. Senthil Kumar R, Ravikumar N, Kavitha S, Mahalaxmi S, Jayasree R, Sampath Kumar TS, et al. Nanochitosan modified glass ionomer cement with enhanced mechanical properties and fluoride release. Int J Biol Macromol. 2017;104(Pt B):1860–5. doi:10.1016/j.ijbiomac.2017.05.120
56. Thenumkal E, Sahoo N, Chopra S, Joshi P, Mustafa M, Kumari D. Evaluation of mechanical properties of chitosan-modified GIC. J Contemp Dent Pract. 2025;26(5):468–72. doi:10.5005/jp-journals-10024-3844
57. Fathi U, Agha M, Ahmad Z. Effect of titanium dioxide nanoparticles on glass ionomer cement. J Res Med Dent Sci. 2022;10:88–91.
58. Sheta MS, Eldin ZE. High-viscosity glass-ionomer cement modified by eucalyptus extract nanoparticles. Odontology. 2026. doi:10.1007/s10266-025-01291-2
59. Tüzüner T, Ulusu T. Effect of antibacterial agents on surface hardness of glass-ionomer cement. J Appl Oral Sci. 2012;20(1):45–9. doi:10.1590/s1678-77572012000100009
60. Garcia-Contreras R, Scougall-Vilchis RJ, Contreras-Bulnes R, Sakagami H, Morales-Luckie RA, Nakajima H. Mechanical, antibacterial, and bond strength properties of nano-titanium-enriched glass ionomer cement. J Appl Oral Sci. 2015;23(3):321–8. doi:10.1590/1678-775720140496
61. Sebastiammal S, Mariappan A, Santhamoorthy M, Elangovan N, Alqhtani HA, Herin RF, et al. Synthesis of titanium oxide modified composites and antibacterial activity. Luminescence. 2025;40(6):e70226. doi:10.1002/bio.70226
62. Ahrari F, Eslami N, Rajabi O, Ghazvini K, Barati S. Antimicrobial sensitivity of Streptococcus mutans to nanoparticles. Dent Res J (Isfahan). 2015;12(1):44–9. doi:10.4103/1735-3327.150330
63. Kini A, G KM, N S, Shetty N, Venkataiah VS, Fareed M, et al. Comparative evaluation of microleakage of restorative materials. Ir J Med Sci. 2025;194(3):1105–11. doi:10.1007/s11845-025-03927-2

64. Elsaka SE, Hamouda IM, Swain MV. Titanium dioxide nanoparticles addition to glass-ionomer restorative. J Dent. 2011;39(9):589–98. doi:10.1016/j.jdent.2011.05.006